

## Inorganic Chemistry

# A Photoionization Study on the Detection of 1-Sila Glycolaldehyde ( $\text{HSiOCH}_2\text{OH}$ ), 2-Sila Acetic Acid ( $\text{H}_3\text{SiCOOH}$ ), and 1,2-Disila Acetaldehyde ( $\text{HSiOSiH}_3$ )

Sankhabrata Chandra,<sup>[a, b]</sup> André K. Eckhardt,<sup>[c]</sup> Andrew M. Turner,<sup>[a, b]</sup> György Tarczay,<sup>[a, d]</sup> and Ralf I. Kaiser<sup>\*[a, b]</sup>

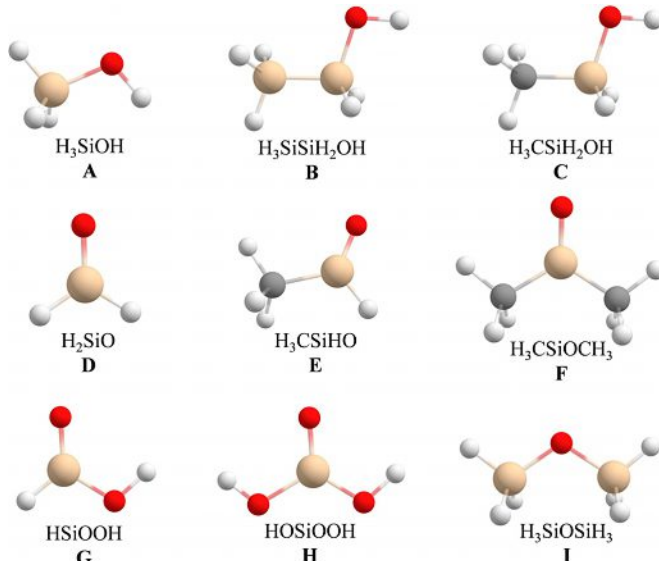
**Abstract:** The identification of silicon-substituted, complex organics carrying multiple functional groups by classical infrared spectroscopy is challenging because the group frequencies of functional groups often overlap. Photoionization (PI) reflectron time-of-flight mass spectrometry (ReTOF-MS) in combination with temperature-programmed desorption (TPD) holds certain advantages because molecules are identified after sublimation from the matrix into the gas phase based on distinct ionization energies and sublimation tem-

peratures. In this study, we reveal the detection of 1-silaglycolaldehyde ( $\text{HSiOCH}_2\text{OH}$ ), 2-sila-acetic acid ( $\text{H}_3\text{SiCOOH}$ ), and 1,2-disila-acetaldehyde ( $\text{H}_3\text{SiSiHO}$ )—the silicon analogues of the well-known glycolaldehyde ( $\text{HCOCH}_2\text{OH}$ ), acetic acid ( $\text{H}_3\text{CCOOH}$ ), and acetaldehyde ( $\text{H}_3\text{CCHO}$ ), in the gas phase after preparation in silane ( $\text{SiH}_4$ )–carbon dioxide ices exposed to energetic electrons and subliming the neutral reaction products formed within the ices into the gas phase.

## Introduction

Ever since the isolation of the first silanol—triethylsilanol ( $(\text{C}_2\text{H}_5)_3\text{SiOH}$ )—by Ladenburg in 1871,<sup>[1]</sup> organosilicon molecules such as silanoles, sialdehydes, silaketones, and silacarboxylic acids carrying the  $\text{Si}=\text{O}-\text{H}$ ,  $-\text{SiHO}$ ,  $-\text{SiO}-$ , and  $-\text{SiOOH}$  functional groups (Scheme 1) have received considerable interest from the (physical) organic, computational chemistry, and synthetic chemistry communities.<sup>[2]</sup> This interest connects to their exploitation as reactive intermediates in organosilicon chemistry<sup>[2]</sup> such as through cross-coupling reactions and their isovalency to alcohols ( $\text{C}=\text{O}-\text{H}$ ), aldehydes ( $-\text{CHO}$ ), ketones ( $-\text{CO}-$ ), and carboxylic acids ( $-\text{COOH}$ ), respectively (Scheme 1). Here, Langmuir's concept of isovalency, in which “two molecular entities with the same number of valence electrons have similar chemistries”,<sup>[3]</sup> has been fundamental in the perception

of basic principles of molecular structures of isovalent systems and in advancing modern concepts of chemical bonding.<sup>[4]</sup> Special attention has been attributed to chemical bonding of reactive intermediates containing main group XIV elements carbon and silicon, which have both four valence electrons. Silicon, unlike carbon, does not easily form silicon–oxygen double bonds,<sup>[5]</sup> but the  $\text{Si}=\text{O}-\text{Si}$  bonds are more stable compared to the  $\text{C}=\text{O}-\text{C}$  moieties due to  $n_{\text{O}} \rightarrow \sigma^*_{\text{Si}}$  interactions.<sup>[6]</sup> In



**Scheme 1.** Key classes of organosilicon molecules prepared in low-temperature ices. Atoms are color coded in red (oxygen), white (hydrogen), gray (carbon, and orange (silicon).

[a] S. Chandra, A. M. Turner, G. Tarczay, R. I. Kaiser

Department of Chemistry, University of Hawaii at Manoa  
2545 McCarthy Mall, Honolulu, HI 96822 (USA)

E-mail: ralfk@hawaii.edu

[b] S. Chandra, A. M. Turner, R. I. Kaiser

W. M. Keck Laboratory in Astrochemistry, University of Hawaii at Manoa  
2545 McCarthy Mall, Honolulu, HI 96822 (USA)

[c] A. K. Eckhardt

Department of Chemistry, MIT, Cambridge, MA 02139 (USA)

[d] G. Tarczay

Present address: Laboratory of Molecular Spectroscopy  
Institute of Chemistry, Eötvös University  
Pázmány Péter sétány 1/A, 1117 Budapest (Hungary)

 Supporting information and the ORCID identification numbers for the authors of this article can be found under:

<https://doi.org/10.1002/chem.202004863>.

a series of matrix isolation studies, Andrews et al. characterized the simplest representatives of silanoles (silamethanol,  $\text{H}_3\text{SiOH}$ , **A**; 1,2-disilaethanol,  $\text{H}_3\text{SiSiH}_2\text{OH}$ , **B**; 1-silaethanol,  $\text{H}_3\text{CSiH}_2\text{OH}$ , **C**), silaaldehydes (silaformaldehyde,  $\text{H}_3\text{SiO}$ , **D**; 1-silaethanal  $\text{CH}_3\text{SiHO}$ , **E**), silaketones (2-sila-2-propanone,  $\text{H}_3\text{CSiOCH}_3$ , **F**), silacarboxylic acids (1-sila-methanoic acid,  $\text{HSiOOH}$ , **G**; 1-sila-carbonic acid,  $\text{HOSiOOH}$ , **H**), and silaethers (1,2-disiladimethylether,  $\text{H}_3\text{SiOSiH}_3$ , **I**) infrared spectroscopically.<sup>[7]</sup> Through reactions of, say, oxygen atoms with silane ( $\text{SiH}_4$ )<sup>[5b]</sup> combined with elegant isotopic substitution experiments, the authors inferred oxygen atom insertion pathways into silicon—hydrogen bonds followed by either stabilization of the reactive silanol intermediate to yield **A** or—by decomposition through hydrogen loss—eventually **D**.

However, despite the ongoing interest in the organosilicon chemistry from the preparative (in)organic and physical chemistry perspectives as isovalent carbon analogous molecules, with the exception of 1,2-disilaethanol ( $\text{H}_3\text{SiSiH}_2\text{OH}$ , **B**) and 1,2-disiladimethylether ( $\text{H}_3\text{SiOSiH}_3$ , **I**), infrared spectroscopic characterization rarely allows an identification of mixtures of silicon-substituted, more complex organics in particular of organosilicon molecules carrying multiple functional groups. This is because *group frequencies* such as of silacarboxylic acids often overlap in the infrared spectrum making a definite assignment of silicon-bearing organics highly challenging.<sup>[8]</sup> Therefore, the lack of preparation and absence of fundamental information on the underlying reaction mechanisms classify multi-functional organosilicon molecules as one of the least explored classes in organosilicon chemistry in gas phase. However, different multifunctional organosilicon molecules are known in solution chemistry.<sup>[9]</sup>

Herein, we report on the preparation and detection of previously elusive 1-sila-glycolaldehyde (1-sila-2-hydroxyethanal,  $\text{HSiOCH}_2\text{OH}$ ), 2-sila acetic acid (2-sila-ethanoic acid,  $\text{H}_3\text{SiCOOH}$ ), and 1,2-disilaacetaldehyde (1,2-disilaethanal,  $\text{H}_3\text{SiSiHO}$ )—the silicon analogues of the well-known glycolaldehyde ( $\text{HCO-CH}_2\text{OH}$ ), acetic acid ( $\text{H}_3\text{CCOOH}$ ), and acetaldehyde ( $\text{H}_3\text{CHCHO}$ ) in the gas phase. Our experimental results are compared with ab initio computed gas phase adiabatic ionization energies. By exposing silane ( $\text{SiH}_4$ )–carbon dioxide ( $\text{CO}_2$ ) ices to energetic electrons and subliming the neutral reaction products formed within the ices into the gas phase, the products were first ionized by a single photon (PI) in the vacuum ultraviolet (VUV) range as obtained by four wave mixing, and eventually mass resolved and detected within a reflectron time-of-flight mass spectrometer (ReTOF-MS). Discrete photon energies at 10.49, 10.10, 9.92, and 9.60 eV along with isotopic substitution experiments were exploited to extract the molecular formulae of the products and to discriminate the structural isomers based on distinct ionization energies thus providing fundamental insights on silicon–silicon and silicon–carbon connectivity together with information on their chemical bonding on previously elusive (organo)silicon molecules.

## Experimental Section

The experiments were performed in a contamination-free ultrahigh vacuum (UHV) stainless steel surface science chamber operated at pressures of a few  $10^{-11}$  Torr using magnetically suspended turbo-molecular pumps coupled with oil-free scroll backing pumps.<sup>[8,10]</sup> In brief, a rhodium-coated silver substrate was interfaced to a two-stage closed-cycle helium cryostat (Sumitomo Heavy Industries, RDK-415E) that can be freely rotated and translated vertically. After the substrate had been cooled to 5 K, silane ( $\text{SiH}_4$ , 99.999%) or  $[\text{D}_4]\text{silane}$  ( $\text{SiD}_4$ , 99% D)–carbon dioxide ( $\text{CO}_2$ , 99.999% or  $\text{C}^{18}\text{O}_2$ , 95%  $^{18}\text{O}$ ) were premixed in a gas mixing chamber at partial pressures of  $65 \pm 1$  Torr (for  $\text{SiH}_4$  or  $\text{SiD}_4$ ) and  $130 \pm 1$  Torr (for  $\text{CO}_2$  or  $\text{C}^{18}\text{O}_2$ ), introduced into the main chamber at a pressure of  $2 \times 10^{-8}$  Torr exploiting a glass capillary array, and deposited onto the substrate. Laser interferometry was used to determine the ice thickness using a helium-neon (HeNe) laser operating at 632.8 nm.<sup>[11,12]</sup> Considering the refractive index of the ices of  $1.3 \pm 0.1$ , a thickness of  $700 \pm 100$  nm was derived. The ratio between the silane and carbon dioxide was determined to be  $1:1 \pm 0.2$  accounting for the integrated absorption coefficients of the  $\nu_3$  mode at  $2181\text{ cm}^{-1}$  for silane of  $4.98 \times 10^{-17}\text{ cm molecule}^{-1}$  and the of the  $\nu_3$  mode at  $2346\text{ cm}^{-1}$  for carbon dioxide of  $7.30 \times 10^{-17}\text{ cm molecule}^{-1}$  (Table S1 in the Supporting Information). The ices were then isothermally irradiated for 60 minutes with 5 keV electrons at a current of 20 nA scanned over an area of  $1.0 \pm 0.1\text{ cm}^2$  at an angle of incidence of  $70^\circ$  relative to the surface normal. To calculate the average penetration depth of the energetic electrons, Monte Carlo simulations (CASINO)<sup>[13]</sup> were carried out yielding an average penetration depth of  $350 \pm 10$  nm and a maximum penetration depth of  $550 \pm 10$  nm (Table S2). Since the penetration depth is less than the thickness of the deposited ices, the energetic electrons only interact with the ices and not with the substrate. On average, the dose is calculated to be  $1.6 \pm 0.2$  eV per  $\text{SiH}_4$  and  $1.1 \pm 0.2$  eV per  $\text{CO}_2$  molecule. During the electron irradiation, the ices were monitored with a Fourier-transform infrared spectrometer (Nicolet 6700) in the range of 6000 to  $600\text{ cm}^{-1}$  at  $4\text{ cm}^{-1}$  resolution accumulating each spectrum over 2 minutes. After the electron irradiation, temperature programmed desorption (TPD) was performed to sublime the ices with the newly formed products. Here, each exposed sample was heated from 5 to 300 K at a rate of  $0.5\text{ K min}^{-1}$ . During TPD, a reflectron time-of-flight mass spectrometer (ReTOF-MS, Jordan TOF Products, Inc.) utilizing photoionization (PI) energies of 10.49, 10.10, 9.92, and 9.60 eV was used to photoionize the subliming molecules. To generate these photon energies, pulsed (30 Hz) coherent vacuum ultraviolet (VUV) light was generated via four-wave mixing using krypton (Specialty Gases, 99.999%) or xenon (Specialty Gases, 99.999%) as a nonlinear medium (Table S3). The VUV light was separated from the fundamentals using a lithium fluoride (LiF) biconvex lens<sup>[14]</sup> (ISP Optics) based on distinct refractive indices of the lens material for different wavelengths.<sup>[15]</sup> The photoionized molecules were extracted, and mass-to-charge ratios were determined on the basis of the arrival time of the ions at a multichannel plate. The signal was amplified with a fast preamplifier (Ortec 9305) and recorded using a bin width of 4 ns, which was triggered at 30 Hz (Quantum Composers, 9518).

## Computational Details

All computations were carried out with Gaussian 16, Revision A.03.<sup>[16]</sup> For geometry optimizations and frequency computations, the density functional theory (DFT) B3LYP functional<sup>[17]</sup> was em-

ployed utilizing the Dunning correlation consistent split valence basis set cc-pVTZ.<sup>[18]</sup> Based on these geometries, the corresponding ab initio frozen-core coupled cluster<sup>[19]</sup> CCSD(T)/cc-pVDZ, CCSD(T)/cc-pVTZ, and CCSD(T)/cc-pVQZ single point energies were computed and extrapolated to complete basis set limit<sup>[20]</sup> CCSD(T)/CBS with B3LYP/cc-pVTZ zero-point vibrational energy (ZPVE) corrections. The adiabatic ionization energies were computed by taking the ZPVE corrected energy difference between the neutral and radical cationic species that correspond to similar conformations. As in general the difference of deuterated and non-deuterated isotopologues in the zero-point vibrational energy is marginal (<0.01 eV), we used the ZPVEs of non-deuterated isotopologues for the adiabatic ionization energy calculation.

## Results and Discussion

### Infrared spectroscopy

Figure 1 displays the FTIR spectra of the silane–carbon dioxide ice before and after the irradiation. Overall, both spectra are dominated by the fundamentals of silane ( $\nu_3$ , 2181 cm<sup>-1</sup>;  $\nu_4$ , 912 cm<sup>-1</sup>) and carbon dioxide ( $\nu_3$ , 2137 cm<sup>-1</sup>;  $\nu_2$ , 662 cm<sup>-1</sup>) along with their combination modes for silane ( $\nu_1 + \nu_3$ , 4292 cm<sup>-1</sup>;  $\nu_2 + \nu_3$ , 3142 cm<sup>-1</sup>;  $\nu_3 + \nu_4$ , 3082 cm<sup>-1</sup>;  $\nu_2 + \nu_4$ , 1868 cm<sup>-1</sup>) and carbon dioxide ( $\nu_1 + \nu_3$ , 3701 cm<sup>-1</sup>;  $2\nu_2 + \nu_3$ , 3594 cm<sup>-1</sup>;  $\nu_3 + \nu_L$ , 2427 cm<sup>-1</sup>; Table S4).<sup>[21]</sup> After the irradiation, new peaks emerged including Si–H and SiH<sub>3</sub> deformation modes at 850 and 930 cm<sup>-1</sup> along with carbonyl (C=O) stretching modes at 1742 and 1704 cm<sup>-1</sup>. The deconvoluted peak of carbon monoxide (CO,  $\nu_1$ , 2142 cm<sup>-1</sup>) is also observable. However, with the exception of carbon monoxide, FTIR cannot identify specific molecules formed in the complex mixtures. Therefore, an alternative analytical approach is required to identify newly formed molecules.

### Photoionization reflectron time-of-flight mass spectrometry

To identify individual molecules formed, photoionization reflectron time-of-flight mass spectrometry (PI-ReToF-MS) was ex-

ploited during the TPD phase of the irradiated ices to 300 K.<sup>[22]</sup> This method represents a unique isomer-selective approach of photoionizing molecules in the gas phase, based on distinct adiabatic ionization energies (IEs) of structural isomers by systematically tuning the photon energies above and below the IE of the isomer(s) of interest. This results in the identification of the parent ions at well-defined mass/charge ratio ( $m/z$ ). Figure 2 represents the PI-ReToF-MS data during the TPD phase of the experiments compiling the temperature-dependence of the ion counts from mass-to-charge ratios ( $m/z$ ) of 10 to 300 over the temperature range from 5 to 300 K. These plots are dominated by higher order silanes (Table S5; Figure S1), which were also reported previously by Tarczay et al. for pure silane ices exposed to energetic electrons.<sup>[23]</sup> These assignments were also confirmed by the isotopically-substituted reactants exploiting [D<sub>4</sub>]silane and C<sup>18</sup>O<sub>2</sub> (Table S5; Figure S1).

Besides the (perdeuterated) silanes, the PI-ReToF-MS data reveal overlapping sublimation profiles for  $m/z$  76. The signal is linked to two possible molecular formulae: SiH<sub>4</sub>CO<sub>2</sub> and Si<sub>2</sub>H<sub>4</sub>O (Figures 3 and 4). The molecular structures of isomers of SiH<sub>4</sub>CO<sub>2</sub> and Si<sub>2</sub>H<sub>4</sub>O along with the computed adiabatic ionization energies at CCSD(T)/CBS/B3LYP/cc-pVTZ + zero-point vibrational energy (ZPVE) and error limits are shown in Figure 4. At 10.49 eV photon energy (Figure 3 A), the TPD profile reveals three sublimation events I–III peaking at 125, 165, and 200 K (Figure 3 A). Let us now untangle the isomers associated with each of these sublimation events. At 10.49 eV, within the error limits, all SiH<sub>4</sub>CO<sub>2</sub> and Si<sub>2</sub>H<sub>4</sub>O isomers can be ionized. Sublimation event I is still visible when the photon energy is lowered to 10.10 eV (Figure 3 B), but it disappears at 9.92 eV (Figure 3 C). As all Si<sub>2</sub>H<sub>4</sub>O isomers have ionization energies below 9.92 eV, they should be ionized if any of isomers 7–9 is formed. Therefore, the lack of ion counts at  $m/z$  76 at 9.92 eV suggests that Si<sub>2</sub>H<sub>4</sub>O molecules do not contribute to the ion counts of the first sublimation event. For SiH<sub>4</sub>CO<sub>2</sub>, isomer 1 can be excluded because it cannot be ionized at 10.10 eV. Likewise, isomers 4–6 can be eliminated; their ionization energies are below 9.92 eV and should reveal ion counts if these isomers

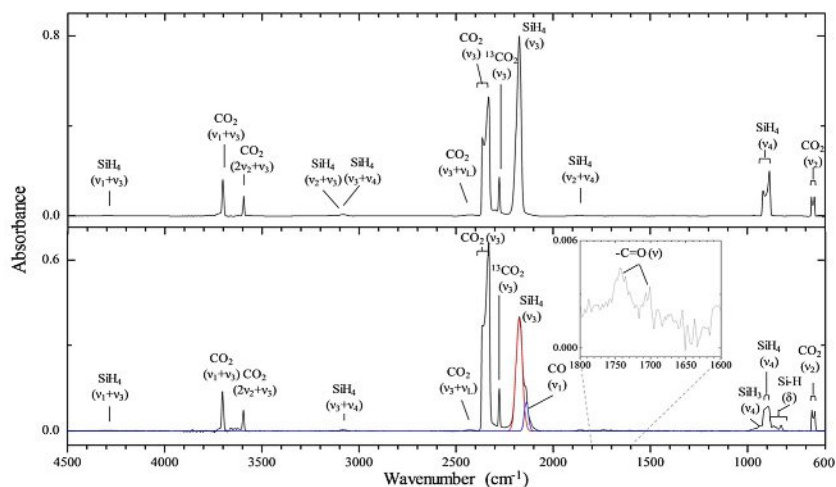


**Figure 1.** Infrared spectra for SiH<sub>4</sub>:CO<sub>2</sub> ices before (top) and after (bottom) 5 keV electron irradiation. The deconvoluted spectra for SiH<sub>4</sub>( $\nu_3$ ) and CO( $\nu_1$ ) are shown in red and blue, respectively.

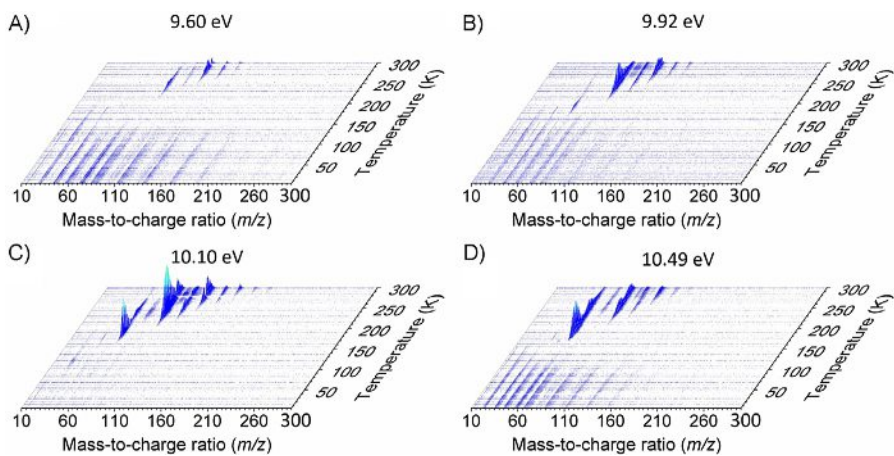


**Figure 2.** Temperature dependent PI-ReTOF-MS data recorded with photon energies A) 9.60, B) 9.92, C) 10.10, and D) 10.49 eV.

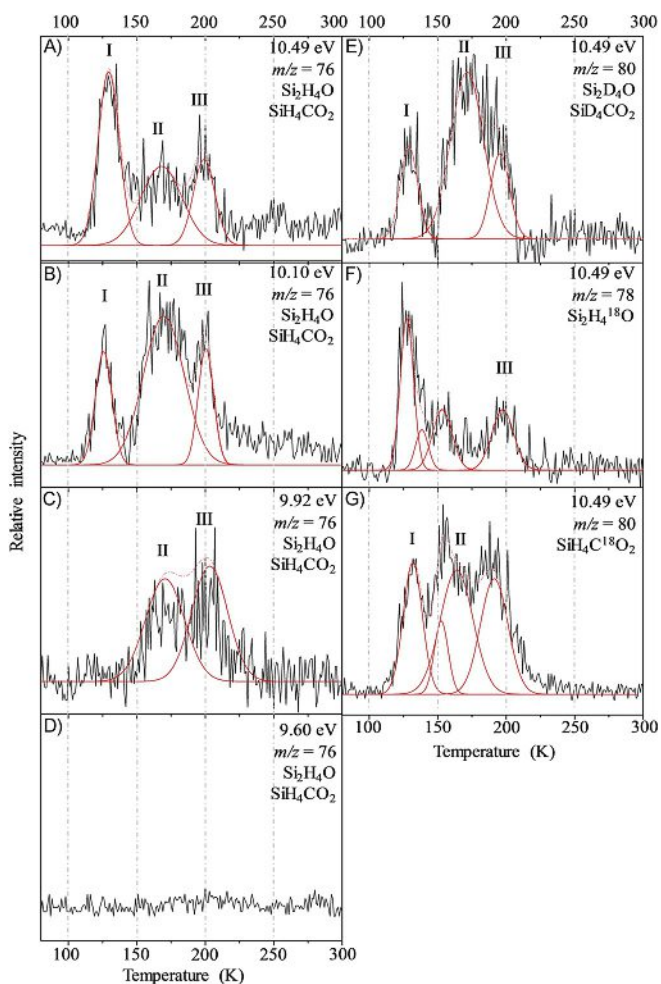


**Figure 3.** Temperature-programmed desorption profiles of the ionized neutral molecules at distinct mass-to-charge ratios subliming from  $\text{SiH}_4:\text{CO}_2$  (A–D),  $\text{SiD}_4:\text{CO}_2$  (E), and  $\text{SiH}_4:\text{C}^{18}\text{O}_2$  ices (F, G). The deconvoluted peaks and the fitted profiles are also shown.

formed. **Therefore, we can conclude that isomer(s) 1-sila-glycolaldehyde **2a–2d** and/or 2-sila acetic acid **3a–3b** contribute to sublimation event I.** The overlapping ranges of ionization energies prevent further identification based on the adia-

batic ionization energies at the present stage. Note that the molecular formula  $\text{SiH}_4\text{CO}_2$  (76 amu) is also supported by the isotopic substitution experiments in  $\text{SiD}_4/\text{CO}_2$  and  $\text{SiH}_4/\text{C}^{18}\text{O}_2$  ices revealing that the first sublimation event is shifted to  $m/z$  80 for  $\text{SiD}_4\text{CO}_2$  and  $\text{SiH}_4\text{C}^{18}\text{O}_2$ , respectively (Figure 3 E and G).

The sublimation event II is present at 10.49, 10.10, and 9.92 eV for the  $\text{SiH}_4/\text{CO}_2$  ices (Figures 3 A–C). However, the equivalent sublimation event is not evident in the exposed  $\text{SiH}_4/\text{C}^{18}\text{O}_2$  ices at  $m/z$  78 ( $\text{Si}_2\text{H}_4^{18}\text{O}$ ; Figure 3 f). Therefore, we can exclude any  $\text{Si}_2\text{H}_4\text{O}$  isomer, and only  $\text{SiH}_4\text{CO}_2$  isomers have to be considered further. This is also supported by the presence of a second sublimation event (165 K) in the  $\text{SiD}_4/\text{CO}_2$  system revealing ion counts shifted to  $m/z$  80 ( $\text{SiD}_4\text{CO}_2$ ; Figure 3 E). Recall that at 10.49 eV, all isomers **1–6** can be ionized; at 10.10 eV, isomer **1** cannot be photoionized and hence can be excluded as a contributor to ion signal at  $m/z$  76 at 10.10 eV. Likewise, at 9.92 eV, isomer **2a** and **2b** cannot be photoionized and therefore, can be eliminated as a contributor to ion signal at  $m/z$  76 at 9.92 eV. Further, at 9.60 eV, no ion signal is present at  $m/z$  76. This allows us to eliminate isomers **4–6** as well. **Consequently, the observable ion counts at 9.92 eV suggest that isomer(s) **3a**, **3b**, **2c**, and/or **2d** are responsible for the second sublimation event.** Once again, the overlapping ranges of ionization energies prevent further identification based on the adiabatic ionization energies at the present stage.

The third sublimation event for  $m/z$  76 is detectable at photon energies of 10.49, 10.10, and 9.92 eV (Figure 3 A–C), but not 9.60 eV (Figure 3 D). This signifies that the third peak cannot be associated with isomers **4–6** of  $\text{SiH}_4\text{CO}_2$  and isomers **8/9** of  $\text{Si}_2\text{H}_4\text{O}$ . Considering the isotopically substituted ices, the third peak at 200 K shifts to  $m/z$  80 for the  $\text{SiD}_4/\text{CO}_2$  system and to  $m/z$  78 for the  $\text{SiH}_4/\text{C}^{18}\text{O}_2$  system. This suggests that the molecule of interest has four hydrogen atoms and one oxygen atom, hence the molecular formula  $\text{Si}_2\text{H}_4\text{O}$ , but not  $\text{SiH}_4\text{CO}_2$ . Consequently, the third sublimation event can be assigned to the  $\text{Si}_2\text{H}_4\text{O}$  isomer **7**—the previously elusive 1,2-disilaacetaldehyde molecule ( $\text{H}_3\text{SiSiHO}$ ).

Having connected (distinct conformers of) isomers **2** and/or **3** ( $\text{SiH}_4\text{CO}_2$ ) to sublimation events I and II as well as the 1,2-di-

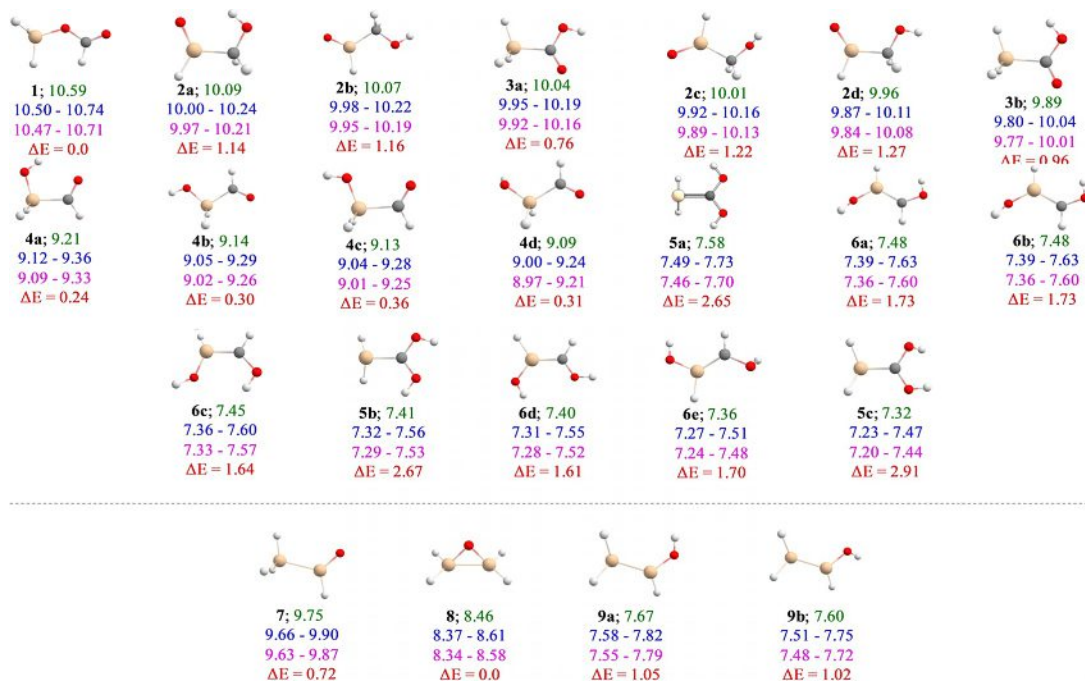


**Figure 4.** Distinct isomers of  $\text{SiH}_4\text{CO}_2$  (top) and  $\text{Si}_2\text{H}_4\text{O}$  (bottom) shown in order of decreasing adiabatic ionization energy. Calculated adiabatic ionization energies (green), ionization energy ranges incorporating the error analysis (blue; Table S6), adiabatic ionization energy ranges corrected for the electric field effect (0.03 eV, pink), and relative energies (red) are shown in eV.

laacetaldehyde molecule ( $\text{H}_3\text{SiSiHO}$ ) 7 to the third sublimation event, we are attempting now to elucidate the origin of sublimation events I and II. To distinguish between 2 and 3, the underlying molecular structures are considered. Isomer 2 represents an alcohol with a silicon-based aldehyde analogue, that is, 1-sila-glycolaldehyde ( $\text{HSiOCH}_2\text{OH}$ ), whereas 3 can be understood in terms of a silylcarboxylic acid: 2-sila acetic acid ( $\text{H}_3\text{SiCOOH}$ ). Previous studies revealed that upon sublimation, carboxylic acids such acetic acid ( $\text{H}_3\text{CCOOH}$ )—the analogue of 3—and formic acid ( $\text{HCOOH}$ ) do not only sublime as monomers, but also as dimers.<sup>[24]</sup> Upon photoionization, this results not only in the molecular ion peak of the monomer (at mass  $M$ ), but also the protonated monomer ( $M+1$ ), the protonated dimer ( $2M+1$ ), the methyl-fragmented dimer ( $2M-15$ ), and the protonated methyl-fragmented dimer ( $2M-14$ ). The sublimation temperatures matched those of the acetic acid monomer indicating that these species could be analogues of acetic acid dimers.<sup>[24a]</sup> These patterns of acetic acid can be transferred to 2-sila acetic acid 3 ( $\text{H}_3\text{SiCOOH}$ ) and assist to distinguish 3 from 2 by analyzing ion signal for the protonated monomer ( $\text{H}_3\text{SiCOOH})\text{H}^+$  ( $m/z$  77), the protonated dimer ( $\text{H}_3\text{SiCOOH})_2\text{H}^+$  ( $m/z$  153), the silyl-fragmented dimer  $\text{H}_3\text{Si}(\text{COOH})_2$  ( $m/z$  121), and the protonated silyl-fragment dimer  $\text{H}_3\text{Si}(\text{COOH})_2\text{H}^+$  ( $m/z$  122). The corresponding TPD profiles for the  $\text{SiH}_4/\text{CO}_2$ ,  $\text{SiD}_4/\text{CO}_2$ , and  $\text{SiH}_4/\text{C}^{18}\text{O}_2$  systems (Figure 5) demonstrate that all (mass shifted) ions connected to 2-sila acetic acid 3 ( $\text{H}_3\text{SiCOOH}$ ) at  $m/z$  77, 121, 122, and 153 are visible for the second sublimation event. Therefore, sublimation event II can be linked to the formation of 2-sila acetic acid 3 ( $\text{H}_3\text{SiCOOH}$ ). On the other hand, critical ion counts are missing for 2-sila acetic acid 3 ( $\text{H}_3\text{SiCOOH}$ ) in the first sublimation event. There-

fore, by principle of exclusion, sublimation event I can be associated with the formation of 1-sila-glycolaldehyde 2 ( $\text{HSiOCH}_2\text{OH}$ ). **To sum up, sublimation events I and II can be linked to two distinct  $\text{SiH}_4\text{CO}_2$  isomers: 1-sila-glycolaldehyde 2 ( $\text{HSiOCH}_2\text{OH}$ ) and 2-sila acetic acid 3 ( $\text{H}_3\text{SiCOOH}$ ), whereas sublimation event III accounts for the formation of a  $\text{Si}_2\text{H}_4\text{O}$  isomer: 1,2-disila acetaldehyde 7 ( $\text{H}_3\text{SiSiHO}$ ).** Note that, as expected for distinct isomers/molecular formulae, the ratios of the three sublimation events of the ion counts at  $m/z$  76 for 10.49, 10.10, and 9.92 eV also differ strongly, that is,  $48 \pm 1:45 \pm 1:3 \pm 1$  (I),  $22 \pm 1:48 \pm 1:15 \pm 1$  (II), and  $27 \pm 1:40 \pm 1:18 \pm 1$  (III), thus reinforcing the aforementioned findings that each sublimation event is linked to a different molecule. Finally, we would like to note that prominent ion signal was also observed at  $m/z$  60 ( $\text{SiH}_4\text{CO}$ ), but overlapping ranges of ionization energies hindered a discrimination between the 2-sila acetaldehyde 11 ( $\text{H}_3\text{SiCHO}$ ) and 1-sila ethylene oxide 12 ( $c\text{-SiH}_2\text{CH}_2\text{O}$ ) isomers (see the Supporting Information).

### Reaction mechanisms

With the identification of three previously elusive organosilicon molecules 1-sila-glycolaldehyde 2 ( $\text{HSiOCH}_2\text{OH}$ ), 2-sila acetic acid 3 ( $\text{H}_3\text{SiCOOH}$ ), and 1,2-disilaacetaldehyde 7 ( $\text{H}_3\text{SiSiHO}$ ), we are proposing now the underlying mechanisms of their formation. Experiments in pure silane ices revealed that the silane molecule decomposes upon interaction with energetic electrons to the silyl radical and atomic hydrogen [Reaction (1)]:<sup>[23a]</sup> The reaction energy for the decomposition from silane to silyl radical and atomic hydrogen is  $+386 \text{ kJ mol}^{-1}$ .<sup>[23b]</sup>

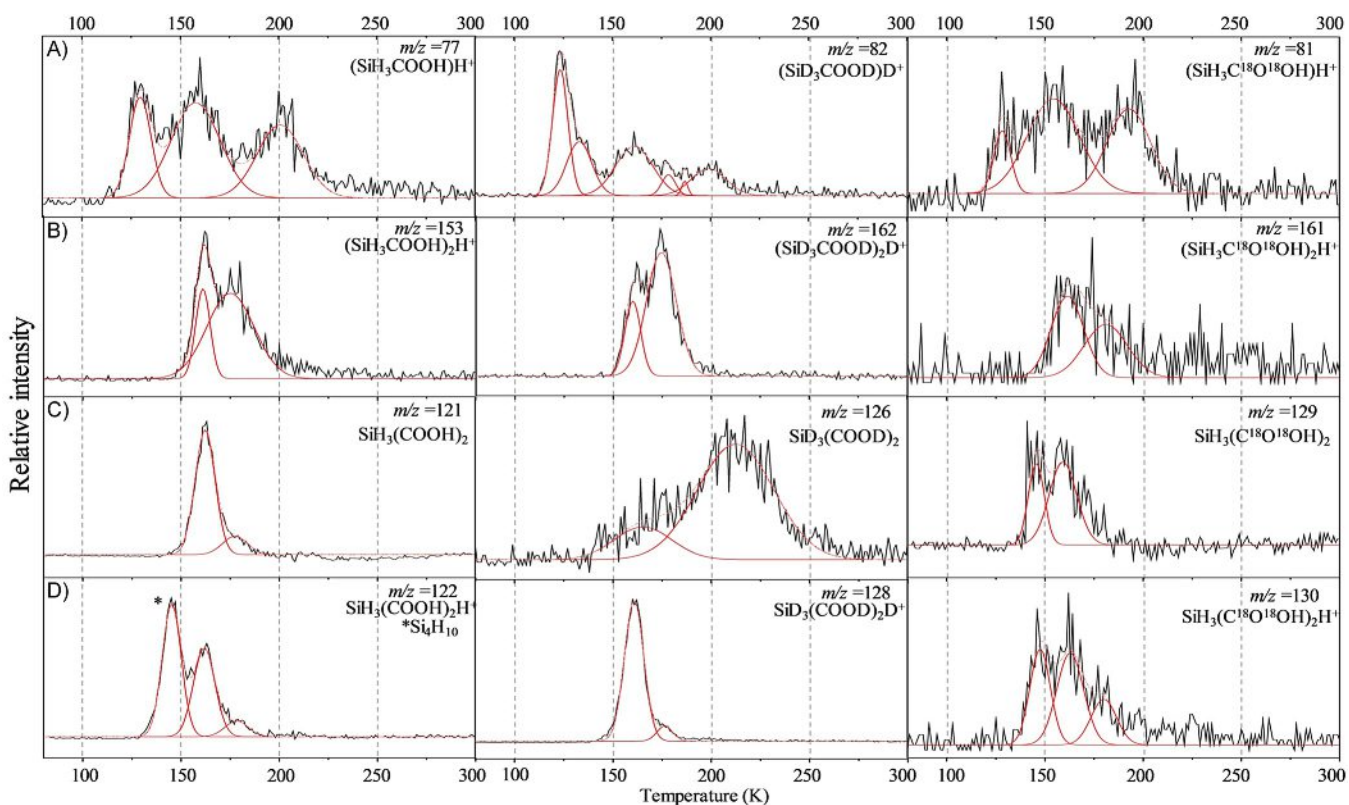


**Figure 5.** Temperature-programmed desorption profiles of the ionized neutral molecules at distinct mass-to-charge ratios subliming from  $\text{SiH}_4:\text{CO}_2$  (left),  $\text{SiD}_4:\text{CO}_2$  (center), and  $\text{SiH}_4:\text{C}^{18}\text{O}_2$  (right) ices at a photon energy of 10.49 eV demonstrating that 2-sila acetic acid can be detected as a protonated parent (A), protonated dimer (B), silyl-fragmented dimer (C), and the protonated silyl-fragmented dimer (D).



The suprathermal hydrogen atoms formed can add to the carbon dioxide molecule ( $\text{CO}_2$ ) forming the hydroxycarbonyl radical ( $\text{HOCO}\cdot$ ) according to Reaction (2) passing a barrier of  $106 \text{ kJ mol}^{-1}$ <sup>[22b, 25]</sup>. The overall reaction energy is  $+22 \text{ kJ mol}^{-1}$ .<sup>[25b]</sup> If both the silyl and the hydroxycarbonyl radical are formed in a favorable recombination geometry, they would react barrierlessly to 2-sila acetic acid **3** ( $\text{H}_3\text{SiCOOH}$ ) through Reaction (3).<sup>[23b]</sup> Note that this excess energy can be transferred from the impinging electrons to the reactants.



Further, the decomposition of carbon dioxide ( $\text{CO}_2$ ) by energetic electrons leads to carbon monoxide and atomic oxygen either in its electronic ground or first excited state (Reaction (4)).<sup>[21b, 26]</sup> This reaction is endoergic by  $532 \text{ kJ mol}^{-1}$  for the triplet channel and by  $732 \text{ kJ mol}^{-1}$  for the singlet channel.<sup>[22b]</sup> Andrews et al. revealed that silane can be oxidized via reactive radical intermediates leading to sila formaldehyde ( $\text{H}_3\text{SiO}$ ), the silaformyl radical ( $\text{HSiO}\cdot$ ), and silicon monoxide ( $\text{SiO}$ ).<sup>[7c,d]</sup> The silaformyl radical may react with the silyl radical to form 1,2-disila acetaldehyde **7** [ $\text{H}_3\text{SiHSiO}$ ; Reaction (5)].



Finally, 1-sila-glycolaldehyde **2** ( $\text{HSiOCH}_2\text{OH}$ ) could be formed—in analogy to the glycolaldehyde molecule ( $\text{HCO-CH}_2\text{OH}$ )<sup>[15, 27]</sup>—via the barrierless radical–radical reaction of silaformyl ( $\text{HSiO}\cdot$ ) with hydroxymethyl [ $\cdot\text{CH}_2\text{OH}$ ; Reaction (6)], which in turn is the result of a step-wise hydrogenation of  $\text{CO}$ .<sup>[28]</sup>



## Conclusions

Using vacuum ultraviolet photoionization reflectron time-of-flight mass spectrometry (PI-ReTOF-MS), this study provides compelling evidence of the generation of three previously elusive organosilicon molecules 1-sila glycolaldehyde ( $\text{HSiO-CH}_2\text{OH}$ ; **2**), 2-sila acetic acid ( $\text{H}_3\text{SiCOOH}$ ; **3**), and 1,2-disila acetaldehyde ( $\text{H}_3\text{SiHSiO}$ ; **7**) in silane–carbon dioxide ices exposed to energetic electrons. These molecules were also identified through their isotope shifts in deuterated and  $^{18}\text{O}$ -substituted samples along with the fragment-free nature and inherent stability of the molecular ion upon ionization of the neutral parent molecule. In addition, ab initio computations were performed to verify the stability of these molecules (minima vs. transition states) and to compute the adiabatic ionization energy exploited in the differentiation of distinct molecules

and isomers through their ionization energies and sublimation temperatures. The application of PI-ReTOF-MS is expected to lead to the identification of further complex silicon molecules, which cannot be identified by traditional methods such as infrared spectroscopy due to overlapping functional groups, in complex icy mixtures obtained from their exposure to ionizing radiation. This will lead to a better understanding of the stabilities, molecular structures, and potential formation pathways of hitherto elusive silicon-carrying molecules.

## Acknowledgements

The experimental work was supported by the U.S. National Science Foundation (NSF) under Award CHE-1853541. A.K.E. thanks the Alexander von Humboldt Foundation for a Feodor Lynen Research Fellowship. G.T. acknowledges Fulbright Foundation.

## Conflict of Interests

The authors declare no conflict of interests.

**Keywords:** gas phase · glycolaldehydes · mass spectrometry · organosilicons · sublimation

- [1] A. Ladenburg, *J. Chem. Soc.* **1872**, *25*, 133–156.
- [2] a) V. Chandrasekhar, R. Boomishankar, S. Nagendran, *Chem. Rev.* **2004**, *104*, 5847–5910; b) M. P. Luecke, E. Pens, S. Yao, M. Driess, *Chem. Eur. J.* **2020**, *26*, 4500–4504; c) D. Wendel, D. Reiter, A. Porzelt, P. J. Altmann, S. Inoue, B. Rieger, *J. Am. Chem. Soc.* **2017**, *139*, 17193–17198; d) N. Tokitoh, R. Okazaki, *Adv. Organomet. Chem.* **2001**, *47*, 121–166.
- [3] I. Langmuir, *J. Am. Chem. Soc.* **1919**, *41*, 868–934.
- [4] a) D. Bellus, *Science of Synthesis: Houben–Weyl Methods of Molecular Transformations* **2000**; b) D. S. N. Parker, A. M. Mebel, R. I. Kaiser, *Chem. Soc. Rev.* **2014**, *43*, 2701–2713.
- [5] a) T. Kudo, S. Nagase, *J. Phys. Chem.* **1984**, *88*, 2833; b) M. M. Linden, H. P. Reisenauer, D. Gerbig, M. Karni, A. Schäfer, T. Müller, Y. Apeloig, P. R. Schreiner, *Angew. Chem. Int. Ed.* **2015**, *54*, 12404–12409; *Angew. Chem.* **2015**, *127*, 12581–12586; c) R. Kobayashi, S. Ishida, T. Iwamoto, *Angew. Chem. Int. Ed.* **2019**, *58*, 9425–9428; *Angew. Chem.* **2019**, *131*, 9525–9528.
- [6] F. Weinhold, R. West, *Organometallics* **2011**, *30*, 5815–5824.
- [7] a) R. Withnall, L. Andrews, *J. Phys. Chem.* **1985**, *89*, 3261; b) R. Withnall, L. Andrews, *J. Am. Chem. Soc.* **1986**, *108*, 8118; c) R. Withnall, L. Andrews, *J. Phys. Chem.* **1988**, *92*, 594; d) R. Withnall, L. Andrews, *J. Am. Chem. Soc.* **1985**, *107*, 2567.
- [8] M. J. Abplanalp, M. Förstel, R. I. Kaiser, *Chem. Phys. Lett.* **2016**, *644*, 79–98.
- [9] B. R. Yoo, N. Jung, *Adv. Organomet. Chem.* **2004**, *50*, 145–177.
- [10] B. M. Jones, R. I. Kaiser, *J. Phys. Chem. Lett.* **2013**, *4*, 1965–1971.
- [11] O. S. Heavens, *Optical Properties of Thin Solid Films*, Scientific Publications Butterworths, London, **1965**.
- [12] P. Groner, I. Stolkin, H. H. J. Gunthard, *Phys. E: Sci. Instrum.* **1973**, *6*, 122–123.
- [13] D. Drouin, A. R. Couture, Joly, D. X. Tastet, V. Aimez, R. Gauvin, *Scanning* **2007**, *29*, 92–101.
- [14] W. A. VonDrasek, S. Okajima, J. P. Hessler, *Appl. Opt.* **1988**, *27*, 4057–4061.
- [15] S. Maity, R. I. Kaiser, B. M. Jones, *Faraday Discuss.* **2014**, *168*, 485–516.
- [16] Gaussian 16, Revision A.03, M. J. Frisch, G. W. Trucks, H. B. Schlegel, G. E. Scuseria, M. A. Robb, J. R. Cheeseman, G. Scalmani, V. Barone, G. A. Petersson, H. Nakatsuji, X. Li, M. Caricato, A. V. Marenich, J. Bloino, B. G. Janesko, R. Gomperts, B. Mennucci, H. P. Hratchian, J. V. Ortiz, A. F. Izmaylov, J. L. Sonnenberg, D. Williams-Young, F. Ding, F. Lipparini, F. Egidi, J. Goings, B. Peng, A. Petrone, T. Henderson, D. Ranasinghe, V. G. Zakrzewski, J. Gao, N. Rega, G. Zheng, W. Liang, M. Hada, M. Ehara, K. Toyota, R. Fukuda, J. Hasegawa, M. Ishida, T. Nakajima, Y. Honda, O. Kitao, H. Nakai, T. Vreven, K. Throssell, J. A. Montgomery, Jr., J. E. Peralta, F. Ogliaro, M. J. Bearpark, J. J. Heyd, E. N. Brothers, K. N. Kudin, V. N. Staroverov, T. A. Keith, R. Kobayashi, J. Normand, K. Raghavachari, A. P. Renard, J. C. Burant, S. S. Iyengar, J. Tomasi, M. Cossi, J. M. Millam, M. Klene, C. Adamo, R. Cammi, J. W. Ochterski, R. L. Martin, K. Morokuma, O. Farkas, J. B. Foresman, D. J. Fox, Gaussian Inc., Wallingford CT, **2016**.
- [17] a) A. D. Becke, *Phys. Rev. A* **1988**, *38*, 3098–3100; b) A. D. Becke, *J. Chem. Phys.* **1993**, *98*, 5648–5652; c) C. Lee, W. Yang, R. G. Parr, *Phys. Rev. B* **1988**, *37*, 785–789.
- [18] J. Dunning, H. Thom, *J. Chem. Phys.* **1989**, *90*, 1007–1023.
- [19] a) J. Čížek, *J. Chem. Phys.* **1966**, *45*, 4256–4266; b) R. J. Bartlett, J. D. Watts, S. A. Kucharski, J. Noga, *Chem. Phys. Lett.* **1990**, *165*, 513–522; c) K. Raghavachari, *Annu. Rev. Phys. Chem.* **1991**, *42*, 615–642; d) J. F. Stanton, *Chem. Phys. Lett.* **1997**, *281*, 130–134.
- [20] K. A. Peterson, D. E. Woon, T. H. Dunning, *J. Chem. Phys.* **1994**, *100*, 7410–7415.
- [21] a) R. I. Kaiser, Y. Osamura, *Astron. Astrophys.* **2005**, *432*, 559; b) C. J. Bennett, C. Jamieson, A. M. Mebel, R. I. Kaiser, *Phys. Chem. Chem. Phys.* **2004**, *6*, 735–746.
- [22] a) A. M. Turner, M. J. Abplanalp, T. J. Blair, R. Dayuha, R. I. Kaiser, *Astrophys. J. Suppl. Ser.* **2018**, *234*, 6; b) C. Zhu, A. M. Turner, M. J. Abplanalp, R. I. Kaiser, *Astrophys. J. Suppl. Ser.* **2018**, *234*, 15.
- [23] a) G. Tarczay, M. Förstel, P. Maksyutenko, R. I. Kaiser, *Inorg. Chem.* **2016**, *55*, 8776–8785; b) K. Hiraoka, T. Sato, S. Sato, S. Hishiki, K. Suzuki, Y. Takahashi, T. Yokoyama, S. Kitagawa, *J. Phys. Chem. B* **2001**, *105*, 6950–6955.
- [24] a) J. Guan, Y. Hu, H. Zou, L. Cao, F. Liu, X. Shan, L. Sheng, *J. Chem. Phys.* **2012**, *137*, 124308; b) A. Bergantini, C. Zhu, R. I. Kaiser, *Astrophys. J.* **2018**, *862*, 140; c) M. S. Arruda, A. Median, J. N. Sousa, L. A. V. Mendes, R. R. T. Marinho, F. V. Prudente, *J. Chem. Phys.* **2016**, *144*, 141101.
- [25] a) B. M. Jones, R. I. Kaiser, G. Strazzulla, *Astrophys. J.* **2014**, *781*, 85; b) C. J. Bennett, R. I. Kaiser, *Astrophys. J.* **2007**, *660*, 1289.
- [26] a) C. J. Bennett, C. S. Jamieson, R. I. Kaiser, *Phys. Chem. Chem. Phys.* **2010**, *12*, 4032–4050; b) C. J. Bennett, C. P. Ennis, R. I. Kaiser, *Astrophys. J.* **2014**, *794*, 57.
- [27] C. J. Bennett, R. I. Kaiser, *Astrophys. J.* **2007**, *661*, 899–909.
- [28] C. J. Bennett, T. Hama, Y. S. Kim, M. Kawasaki, R. I. Kaiser, *Astrophys. J.* **2011**, *727*, 27–37.

Manuscript received: November 5, 2020

Revised manuscript received: December 1, 2020

Accepted manuscript online: December 25, 2020

Version of record online: February 16, 2021